

# Core Characterization of the Cane Creek Interval in the Paradox Formation from the State 16-2 Well

Solutions for Today | Options for Tomorrow



Thomas Paronish  
Research Geologist  
Geological & Environmental Systems



Rocky Mountain Section AAPG  
July 26, 2022



# Disclaimer



This project was funded by the United States Department of Energy, National Energy Technology Laboratory, in part, through a site support contract. Neither the United States Government nor any agency thereof, nor any of their employees, nor the support contractor, nor any of their employees, makes any warranty, express or implied, or assumes any legal liability or responsibility for the accuracy, completeness, or usefulness of any information, apparatus, product, or process disclosed, or represents that its use would not infringe privately owned rights. Reference herein to any specific commercial product, process, or service by trade name, trademark, manufacturer, or otherwise does not necessarily constitute or imply its endorsement, recommendation, or favoring by the United States Government or any agency thereof. The views and opinions of authors expressed herein do not necessarily state or reflect those of the United States Government or any agency thereof.

# Authors and Contact Information

---



Tom Paronish<sup>1, 2</sup>, Dustin Crandall<sup>1</sup>, Johnathan Moore<sup>1, 2</sup>, Terry McKisic<sup>1</sup>, Natalie Mitchell<sup>1, 2</sup>, Sarah Brown<sup>1, 2</sup>,  
Bryan Tenant<sup>1, 2</sup>, Scott Workman<sup>1, 2</sup>, Eric Edelman<sup>3</sup>, Brian McPherson<sup>3</sup>,  
Rich Esser<sup>3</sup>

<sup>1</sup>National Energy Technology Laboratory

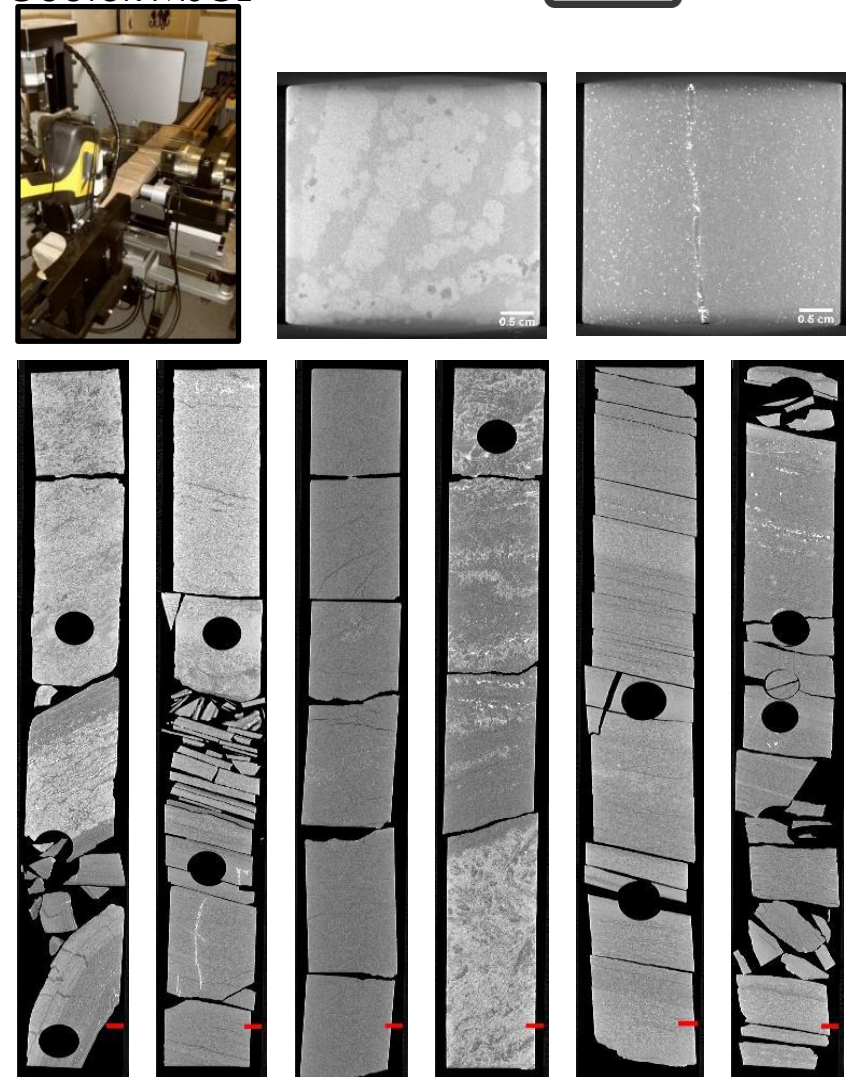
<sup>2</sup>NETL Support Contractor

<sup>3</sup> University of Utah

# Outline

- **NETL Research & Innovation Center Imaging Capabilities and Methods for Core Analysis**
- **Standard Core Characterization**
  - Medical Computed Tomography (CT) Scanning
  - Multi-Sensor Core Logging
- **Sidewall Core Analysis**
  - High-Resolution CT Imaging
  - Permeability as a Function of Effective Stress
  - Xenon and CT Flow Zone Identification
  - Result Tie-In with Core Data

Geotek MSCL

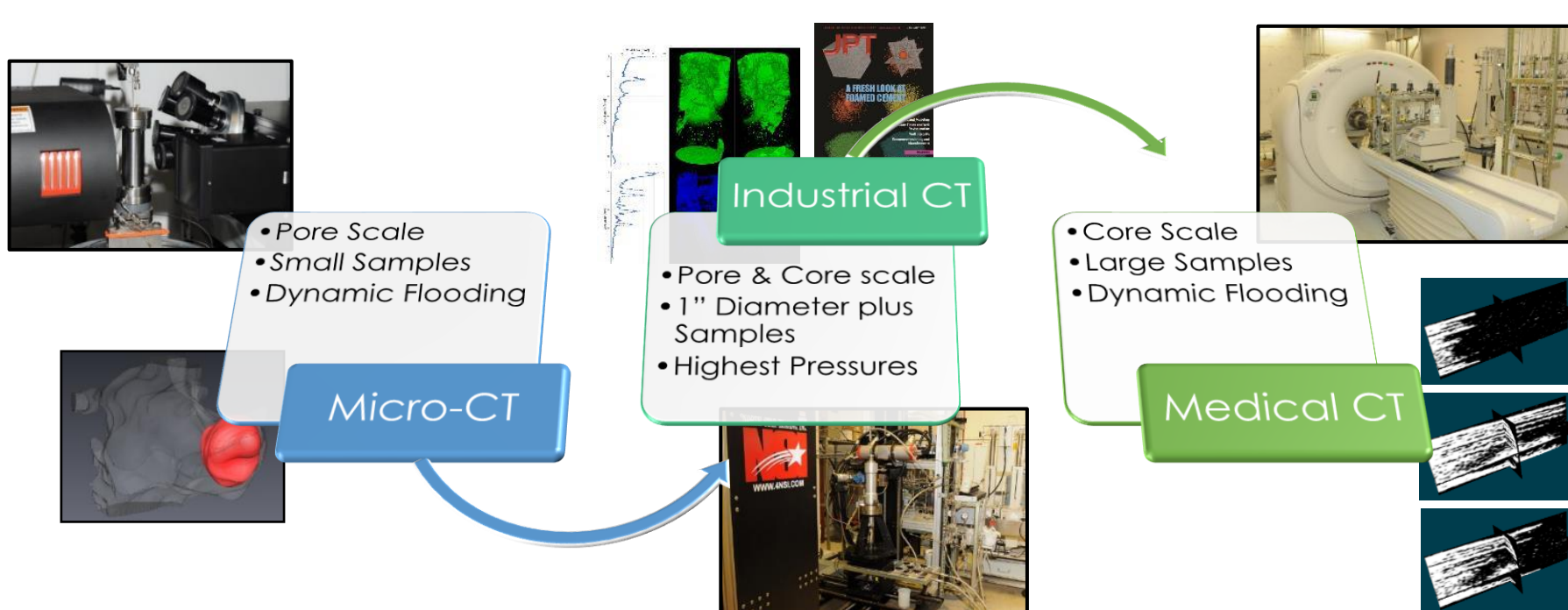


# Multi-Scale CT and Core Flow Facility



**Unique Capabilities:** Four CT scanners with 3D resolution from microns to millimeters, all with ancillary core flow capabilities. Able to perform controlled multiphase flow in cores from 0.25" to 2" in diameter at conditions up to 10,000 psi and 200 °C. Full time technical staff to assist with rock preparation, experimentation design, setup, execution, and analysis. Plus, controlled flow systems for long-term tests, and GeoTek multi-sensor core logger.

**Opportunities:** Direct examination of rocks from carbon storage sites under *in-situ* conditions with supercritical CO<sub>2</sub>. Stressing of samples to understand mechanical behaviors. Examination of relationships between rock properties, geochemical alteration, and permeability (or structural properties). Scanning to complement other experiments, or to digitally and non-destructively preserve core from relevant locations.

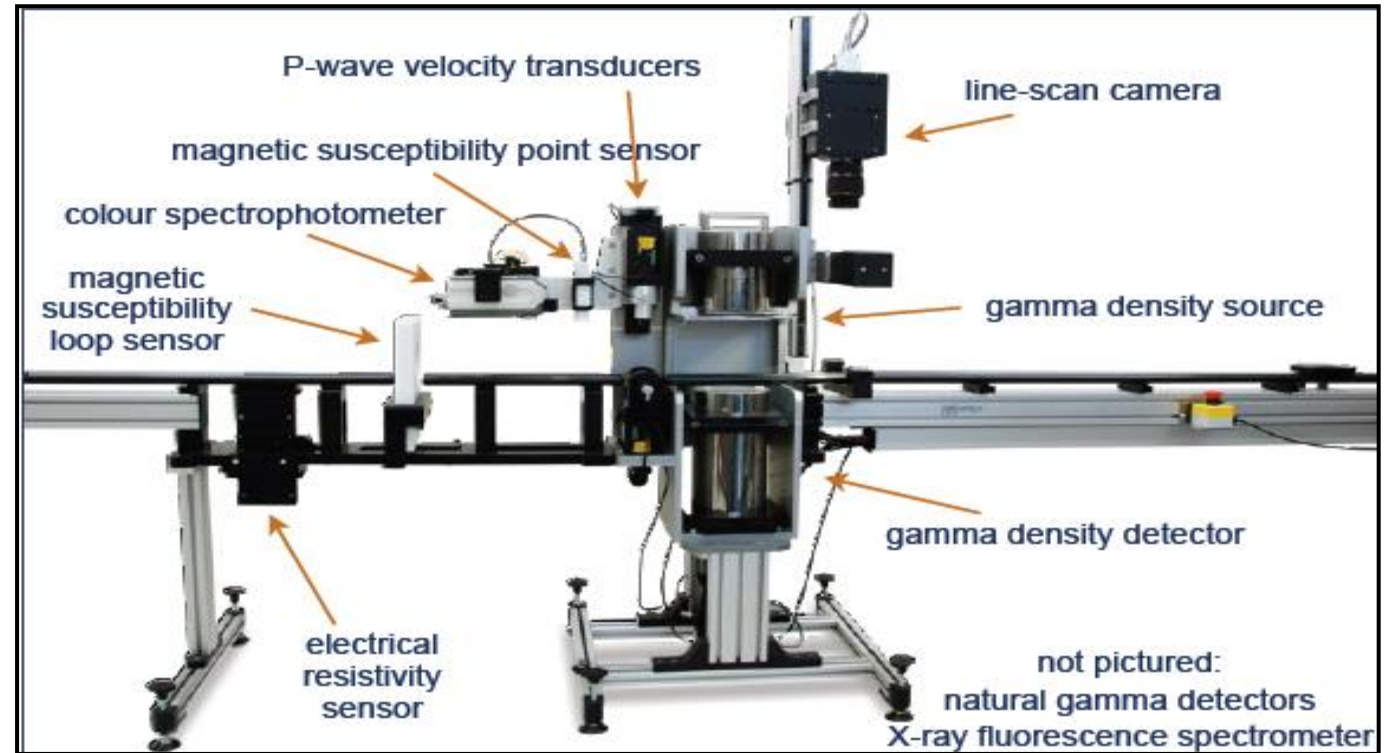


**For More Information:**

- Equipment/Lab Factsheet ([link](#))
- Core characterization EDX Data Group ([link](#))
- Core characterization YouTube Video ([link](#))
- CO<sub>2</sub> Brine Relative Permeability Accessible Database ([link](#))

# Multi-Sensor Core Logger

## Bulk Scans



# Core Logger: Data Acquisition

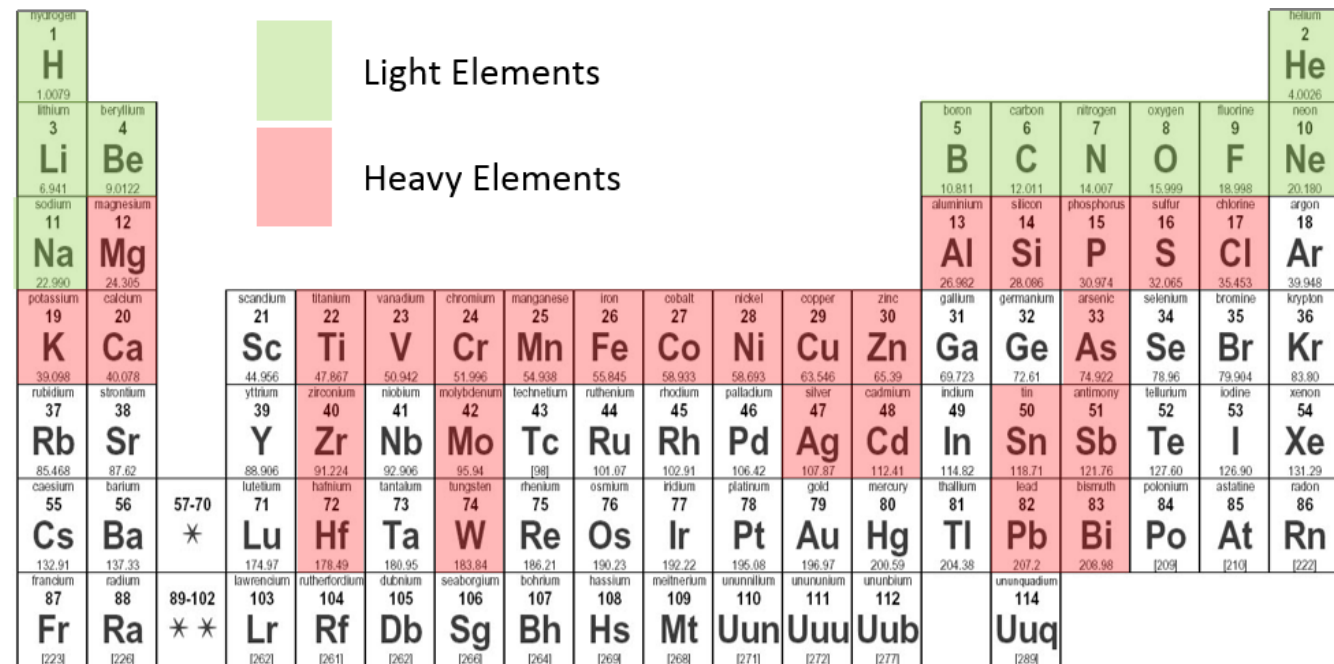
## State 16-2 Well:

## 6 cm sampling resolution

## Data acquired:

# XRF: Mining-plus

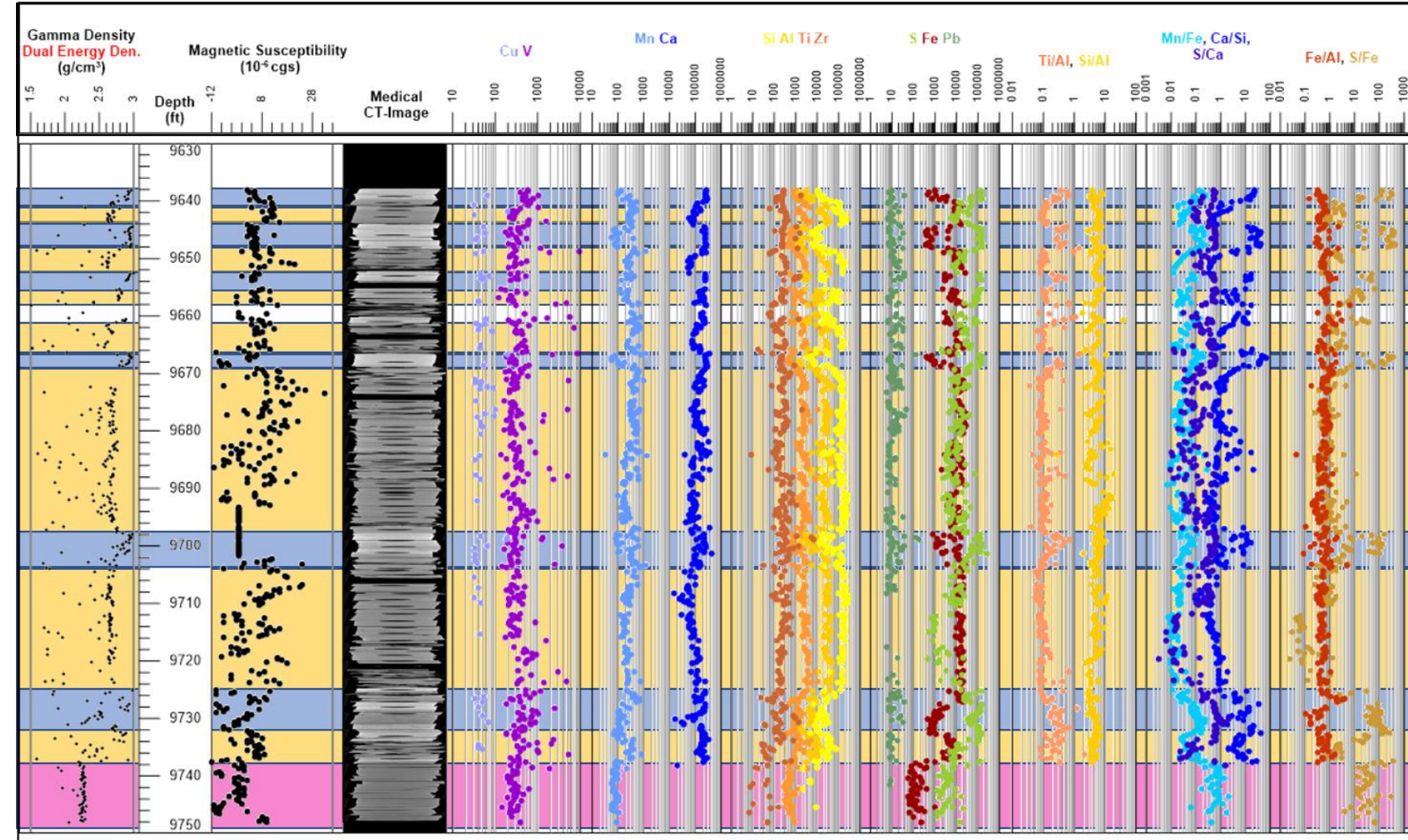
- 60 sec exposure time per beam
- Light elements (LE) in green
- Detection limits: Mg(1%), P(2%), K(2 %),  
Transition metals (1-10 ppm)
- Gamma Density
- Magnetic Susceptibility



# Whole Core: CT Scanned and Logged in the MSCL

Analysis of the XRF shows 3 primary facies:

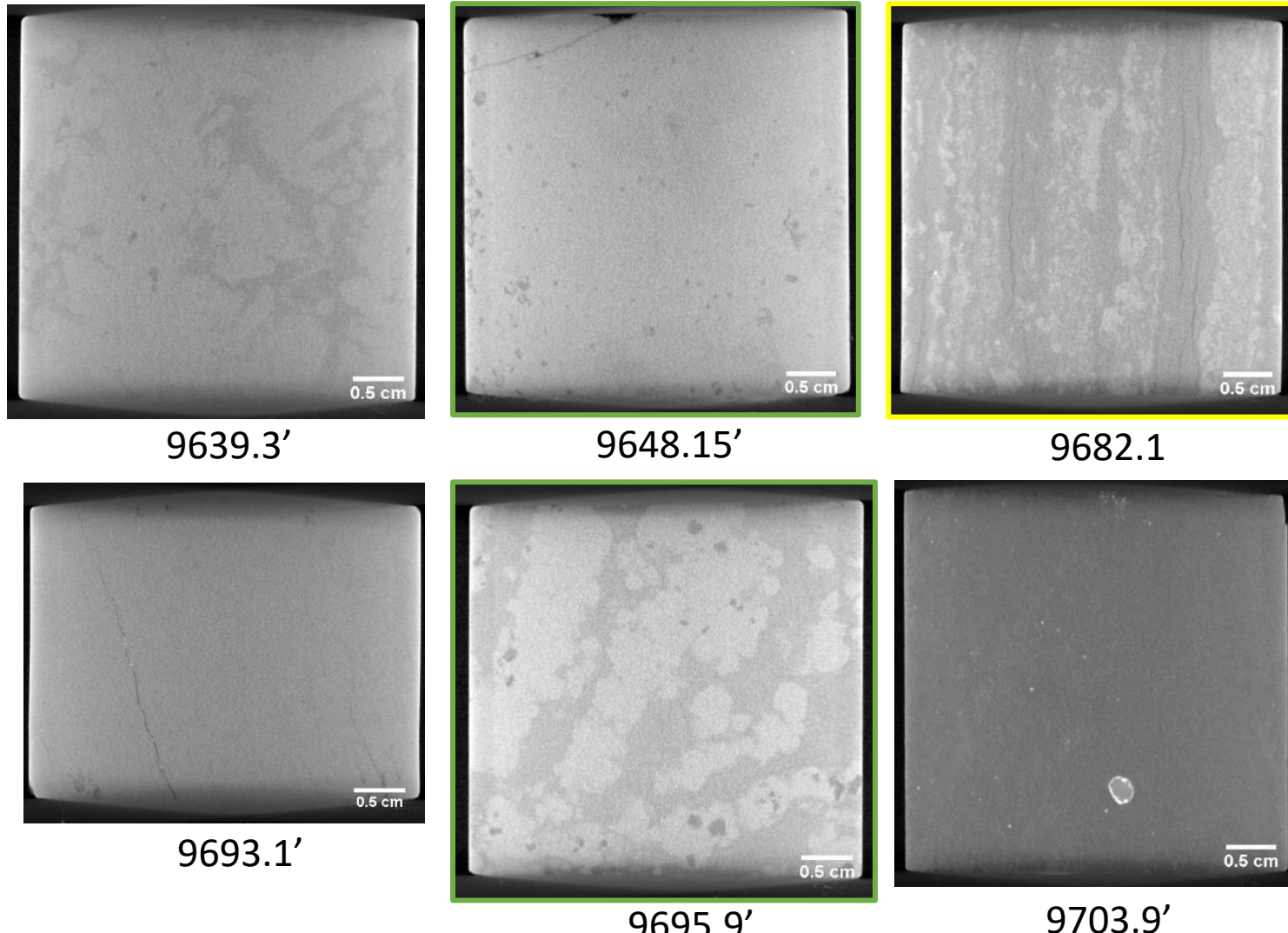
- **Anhydrite-rich zones**
  - Increases in S, Ca, and S/Ca ratio
  - Higher density up to 3 g/cm<sup>3</sup> and decrease in magnetic susceptibility
- **Mudstone/sandy-siltstone:**
  - Enrichment in detrital elements and depletion in S and S/Ca ratio
  - Mudstone portions of the facies occur with an increase in the Ca/Si ratio
- **Halite**
  - Enrichment in Cl and depletion in all other elements
  - Decrease in density and magnetic susceptibility



# Core Plug Analysis: High Resolution CT Imaging



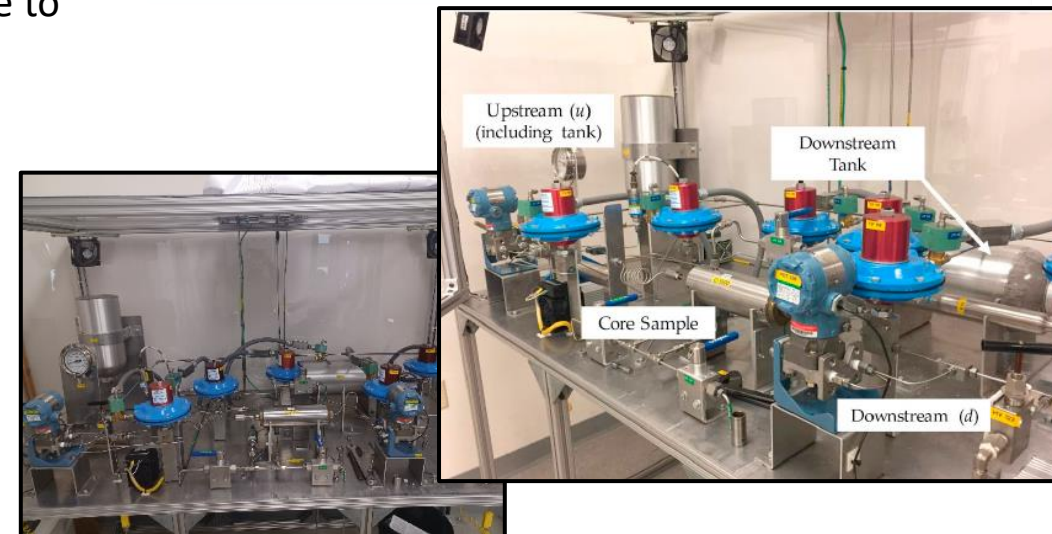
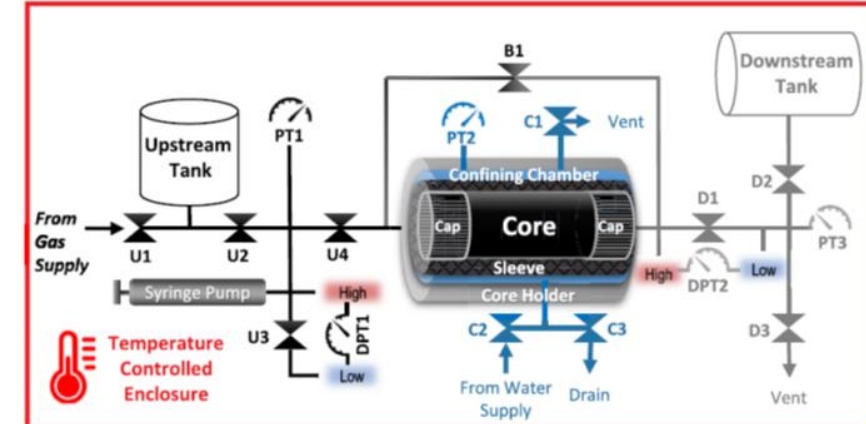
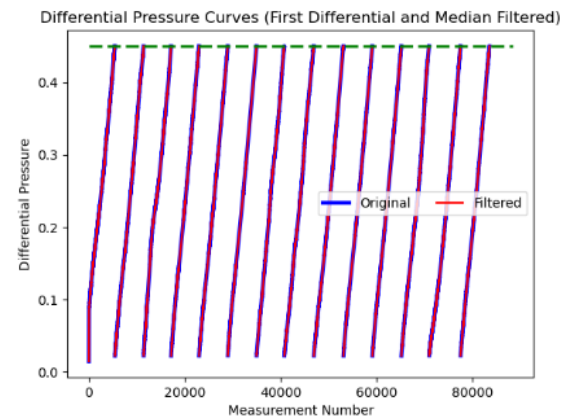
- **TESCAN DynaTOM**
  - Down to 3-micron resolution
  - Very fast scan times
- **Scans were acquired for most of the sidewall cores analyzed for steady-state permeability. Resolution varies; 0.5 cm scale bar is present on the bottom right of the image.**



# Core Plug Analysis: Steady-State Permeability Analysis



- Steady-state permeability measuring device for tight low permeability samples.
- Uses two larger volumes of gas, one on the inlet and one on the outlet, to maintain a constant pressure differential across the core.
- General methodology:
  1. Pressure increases in a small space downstream until it reaches 0.45 psi.
  2. Pressure is released via a valve actuating over a 10 sec period to the downstream reservoir.
  3. The downstream valve is automatically closed and the pressure increase allowed to occur again.
  4. This full process is repeated until the integration time for the pressure to reach 0.45 psi is consistent, “steady-state.”
  5. Permeability is calculated by integrating the rate at which pressure climbs.



Hannon, Michael. *Experimental Data from: Quantifying the Effects of Gaseous Pore Pressure and Net Confining Stress on Low-Permeability Cores Using the "RaSSCAL" Steady-State Permeameter*. Mendeley, 23 May 2019, doi:10.17632/TK6KX5W3MC.

# Permeability Measurements



Peff (psi)	9639.3 - #1		9648.2 - #7		9661.1 - #13		9656 - #11		9658.1 - #12		9663.1 - #14		9664.4 - #15		9665.8 -#17		9670.1 - #20		9695.9 - #37		
	k (nD)	Stdev	k (nD)	Stdev	k (nD)	Stdev	k (nD)	Stdev	k (nD)	Stdev	k (nD)	Stdev	k (nD)	Stdev	k (nD)	Stdev	k (nD)	Stdev	k (nD)	Stdev	
500	3142.58	26.86	467.40	2.73	513.10	7.55	5918.30	157.30			1054.69	7.17								40.76	0.52
1000	2788.42	8.66	261.75	1.47	297.11	18.07	3962.17	73.68			932.52	8.02								24.04	0.54
2000	2359.38	13.30	93.17	9.19	101.35	10.05	971.46	286.18			746.21	14.70	390.08	25.10						20.23	0.39
3200	1542.40	16.18	31.20	X		1.96	X	179.12	31.17			569.92	17.03							15.24	0.34
4500	852.95	15.65	19.27	6.23	0.05	X		65.59	18.47	113.81	1.99	360.25	10.01	6376.11	229.71					8.44	0.40

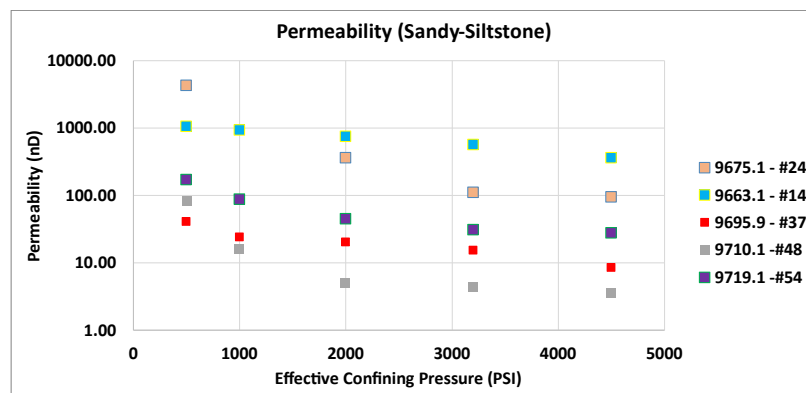
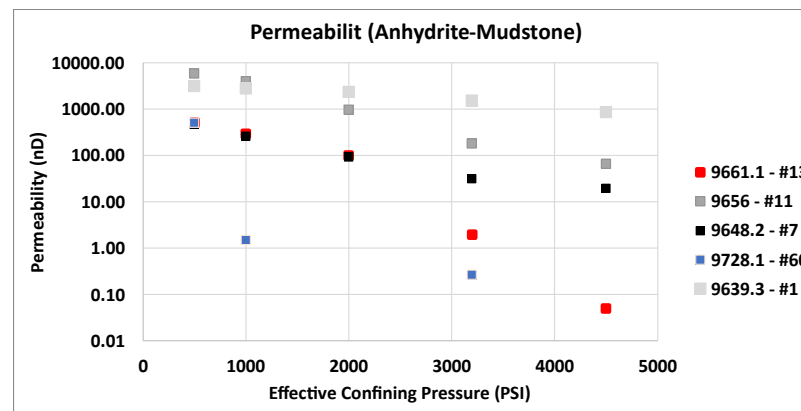
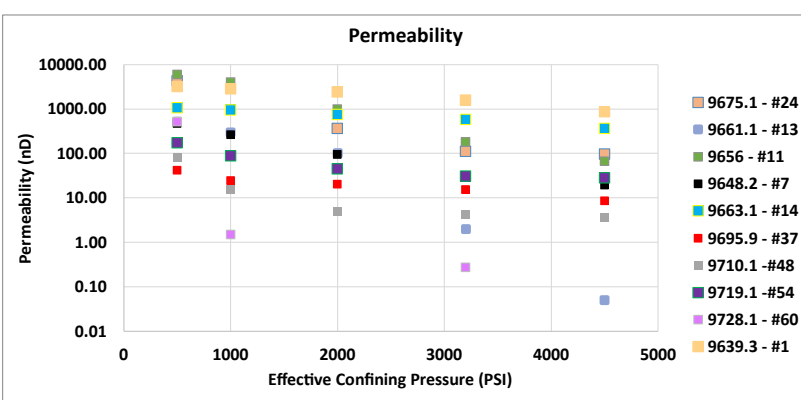
Peff (psi)	9710.1 -#48		9719.1 -#54		9718.1 - #53		9675.1 - #24		9728.1 - #60	
	k (nD)	Stdev	k (nD)	Stdev	k (nD)	Stdev	k (nD)	Stdev	k (nD)	Stdev
500	81.35	39.34	169.71	4.58	105.50	1.04	4257.25	441.85	507.50	68.63
1000	15.84	2.05	87.64	0.63	20.22	1.57			1.48	0.40
2000	4.96	0.15	44.53	2.11	0.47	0.38	363.16	6.50		
3200	4.28	0.30	30.69	2.66			110.73	4.34	0.27	-
4500	3.53	0.20	27.51	1.53			94.94	12.36		



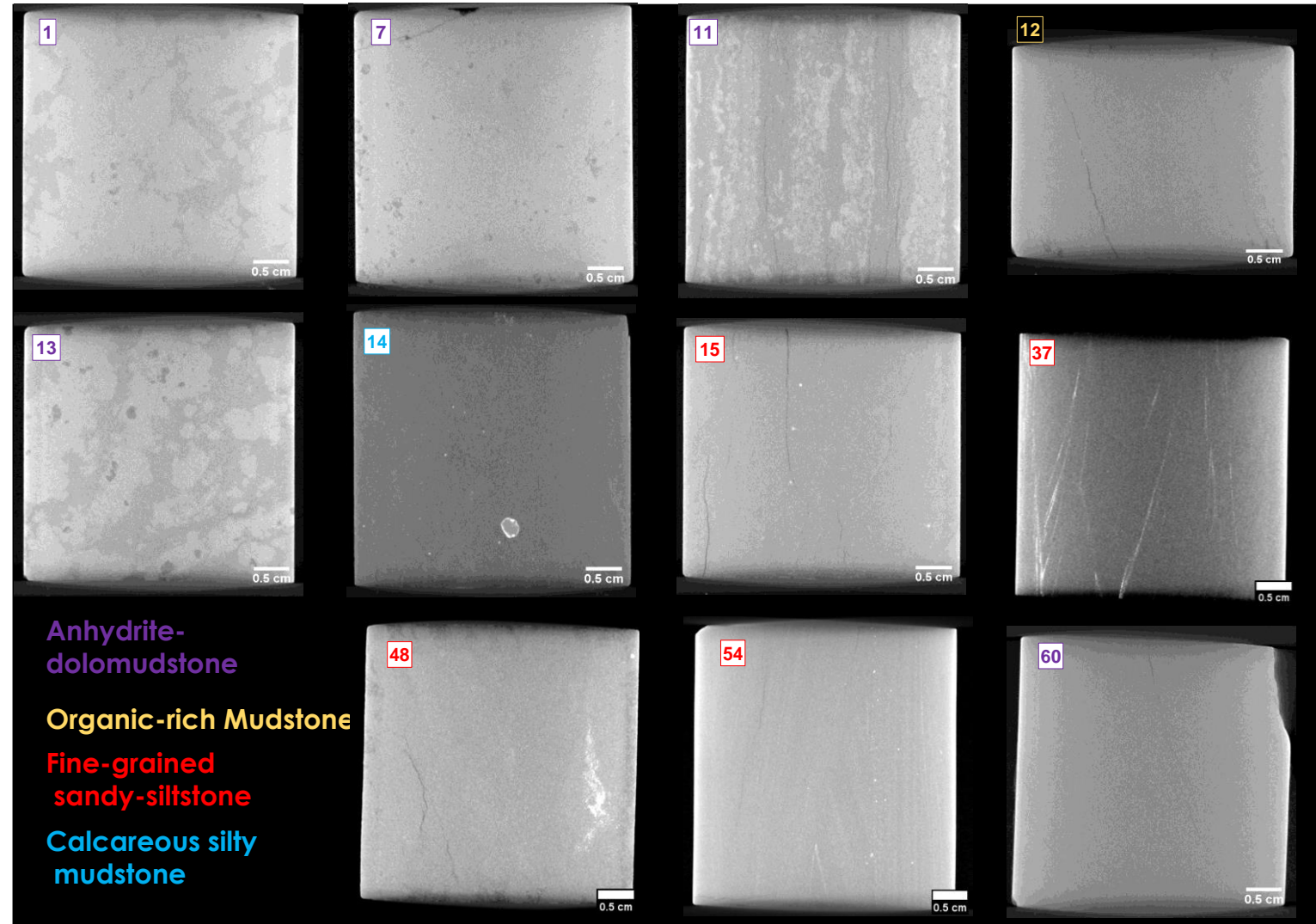
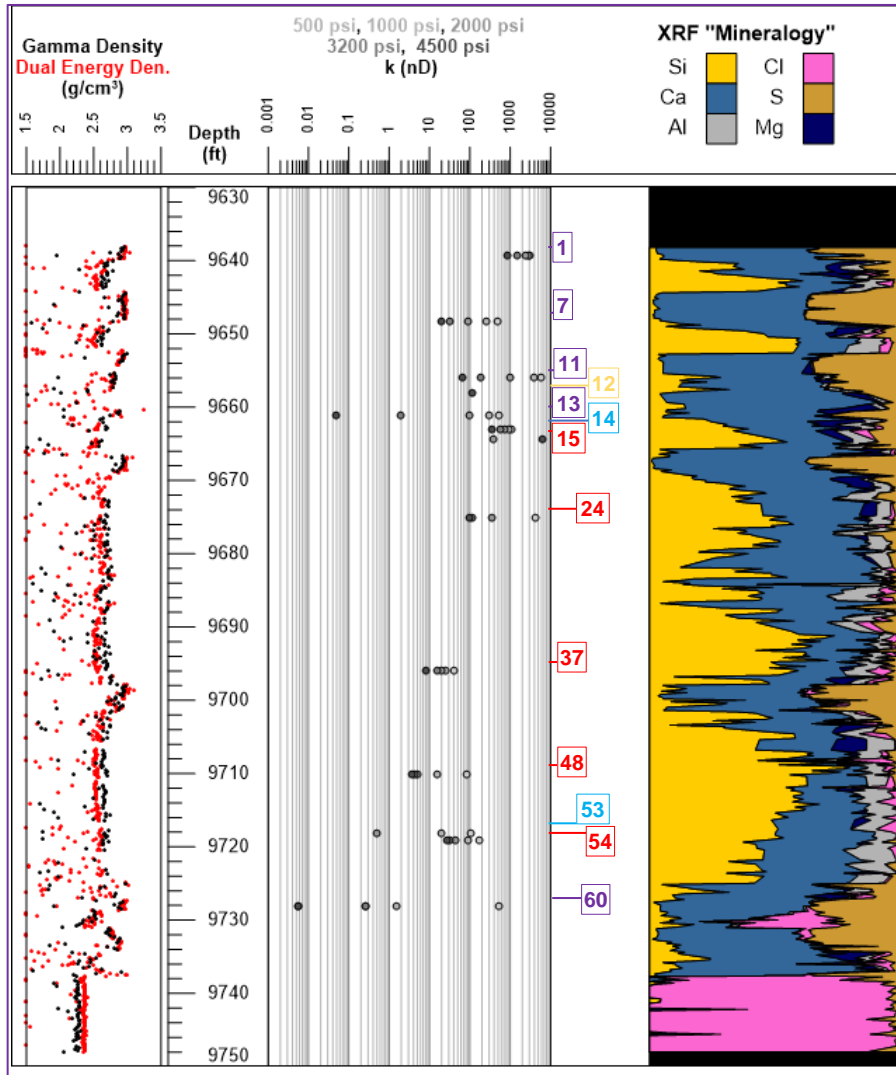
One measurement only



Still in sharp decline when finalized

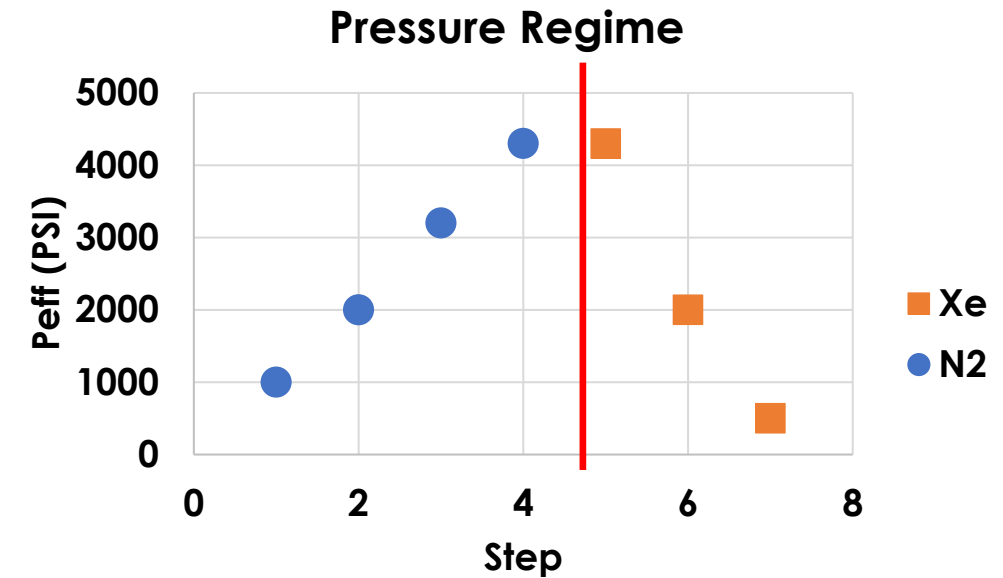
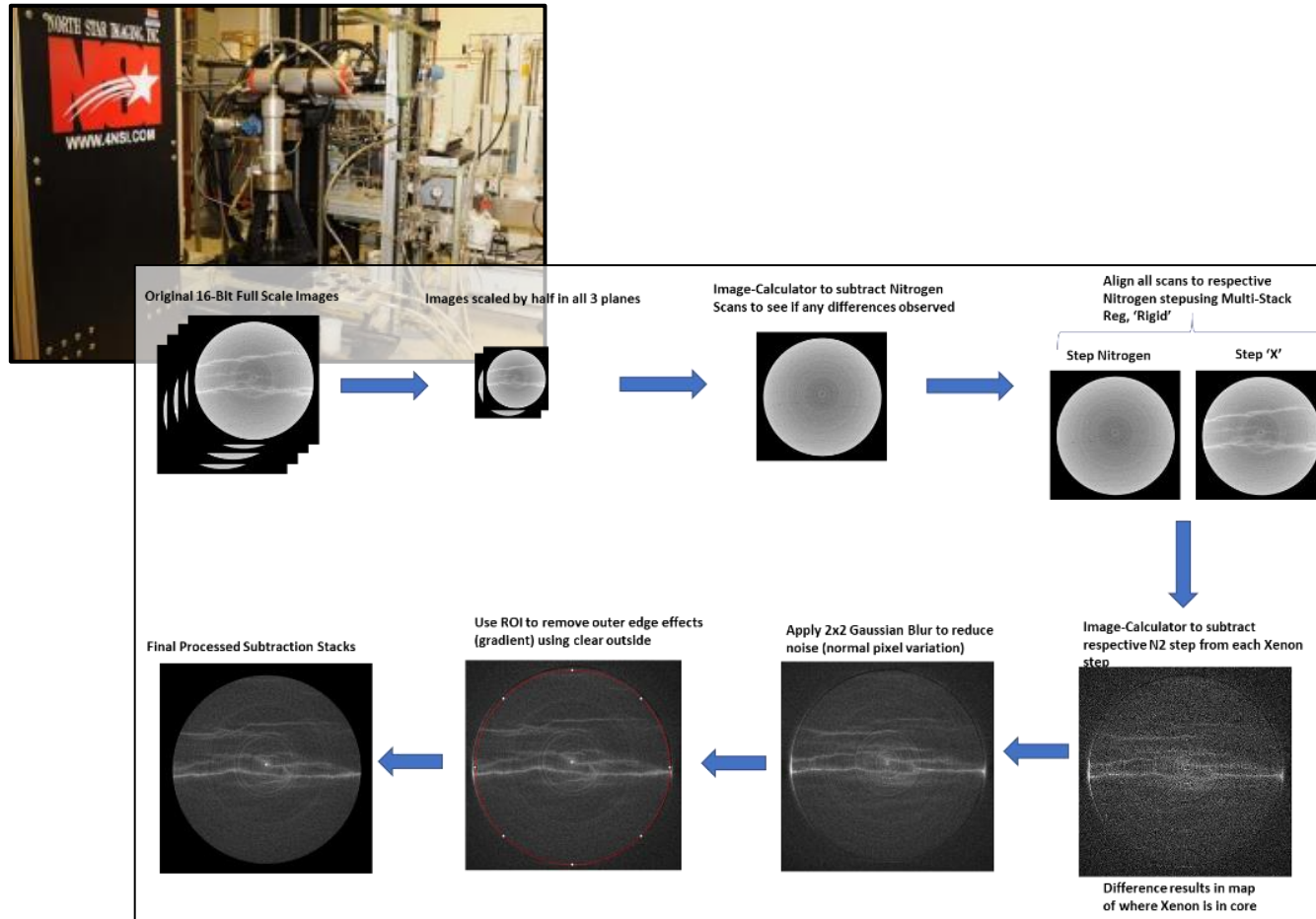


# Permeability Measurements (continued)



# Compression CT Test with Xenon

- Xenon attenuates X-rays significantly; therefore, it is an excellent inert gas to highlight flow pathways (fractures)
- Using core holders and NETL's Industrial CT scanner



- Maintain pore pressure of 600 psi with  $\text{N}_2$
- Slowly raise confining pressure
  - Obtain CT scans at four steps
- Reduce pore **pressure to zero** at  $P_{eff} = 4600$  psi
- Introduce  $\text{Xe}$  to system at **4600 psi**
  - Obtain CT scan
- Lower confining ( $P_{eff}$ ) and CT scan at each step

# Subtraction Images

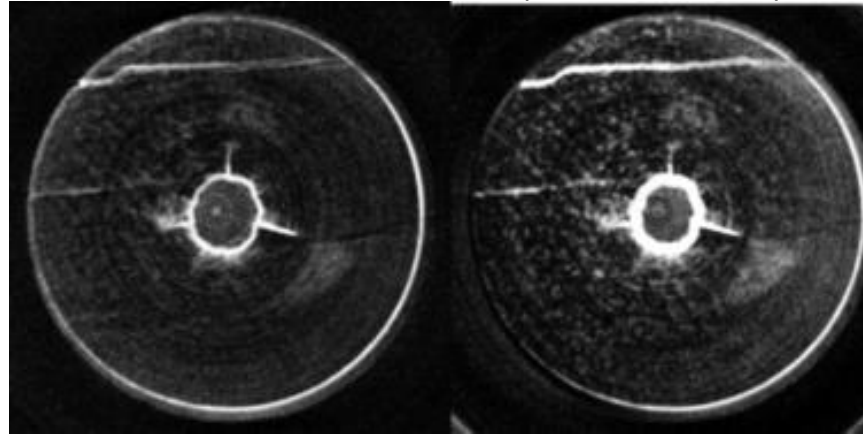
**Top: Bright zones show fractures in the core that close due to increasing effective pressure**

- Pathways apparent with  $N_2$

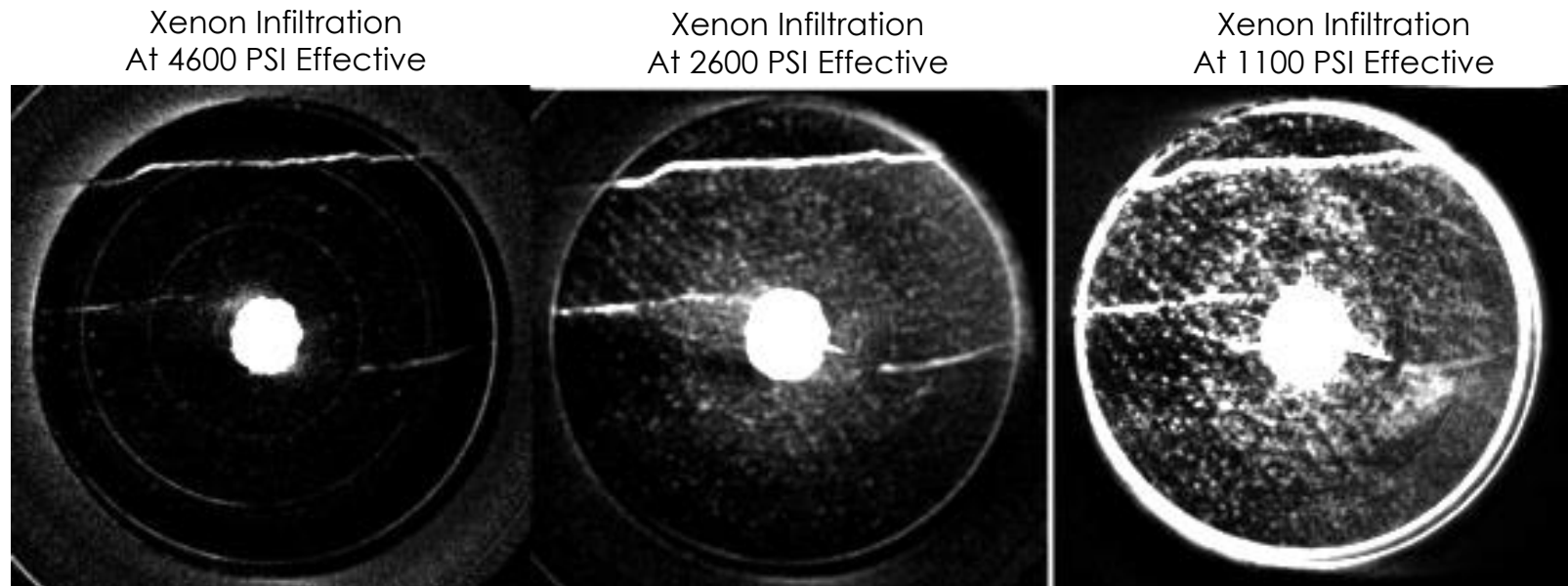
**Bottom:  $Xe$  minus  $N_2$  images at same  $P_{eff}$**

- **Initially, no real change from  $N_2$  scans**
- **Once  $P_{eff} = 1100$  psi significant  $Xe$  in the matrix was observed, but not uniformly**

Fracture Reduction  
(1100 to 2600 PSI)



Fracture Reduction  
(1100 to 5000 PSI)



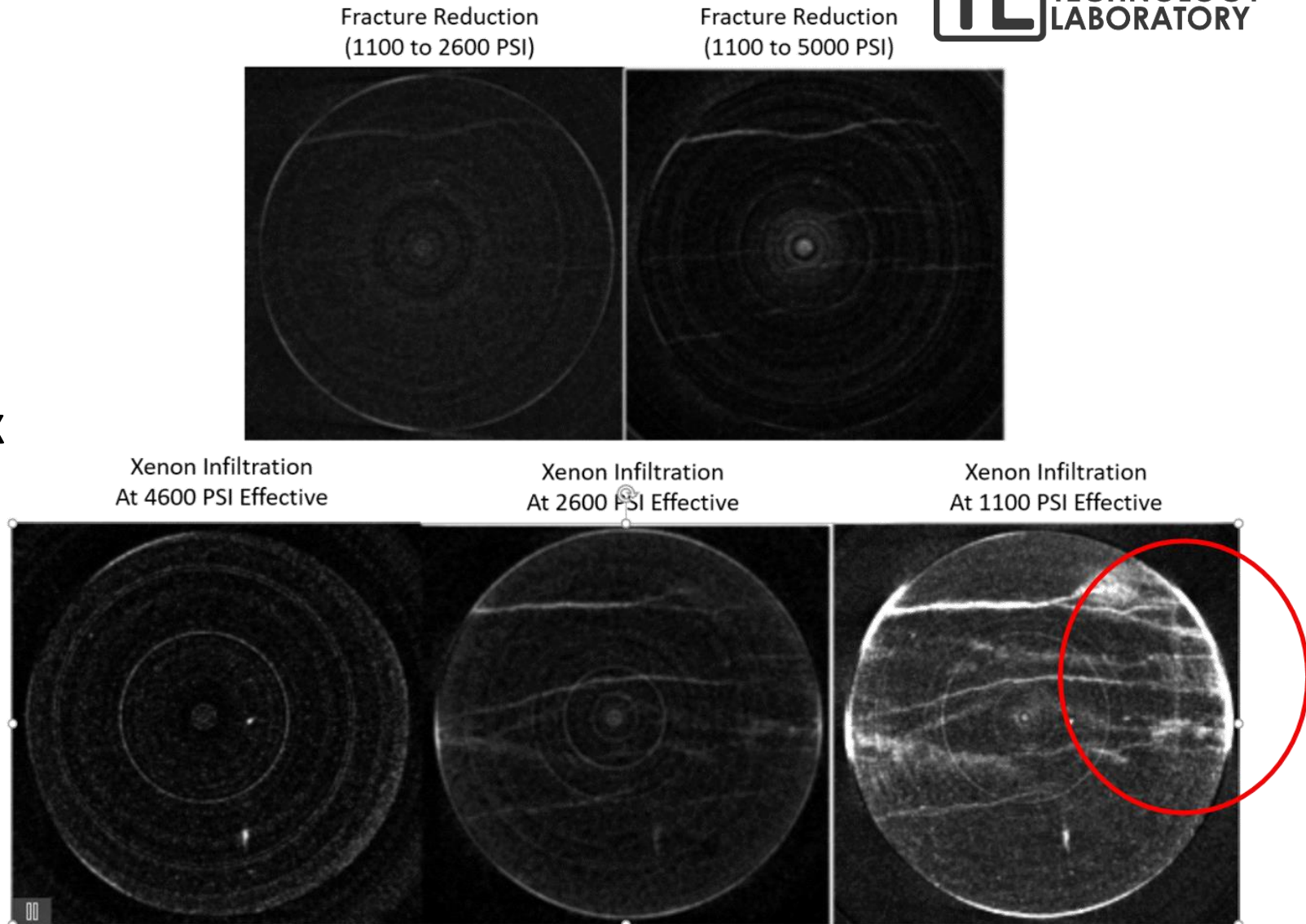
Xenon Infiltration  
At 4600 PSI Effective

Xenon Infiltration  
At 2600 PSI Effective

Xenon Infiltration  
At 1100 PSI Effective

# Fracture Network Analysis

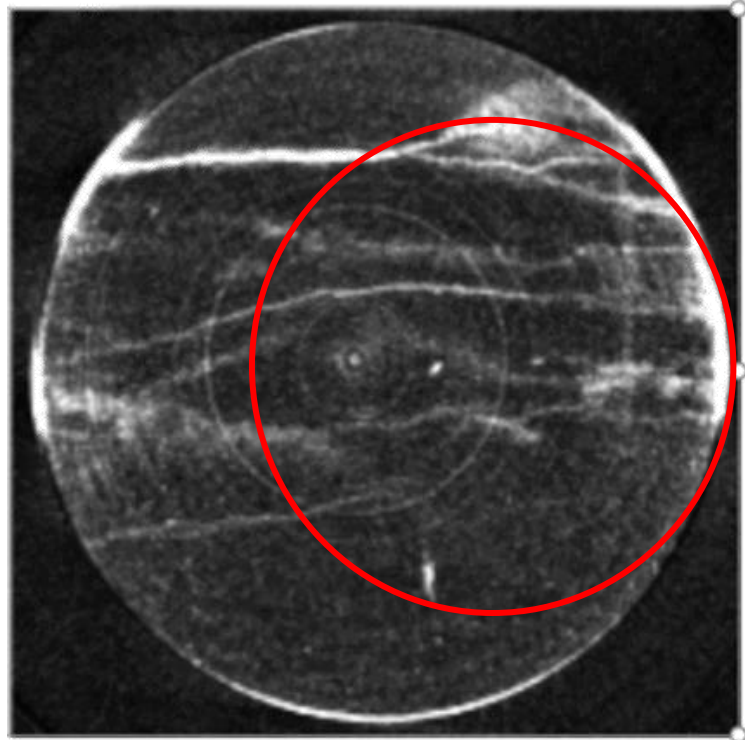
- The non-uniform behavior of the fracture network in response to stress is not surprising
- The *very* localized flow into portions of the matrix is surprising
- Need to further examine what is different about these zones
  - Damaged below resolution of scans?
  - Different mineralogy?



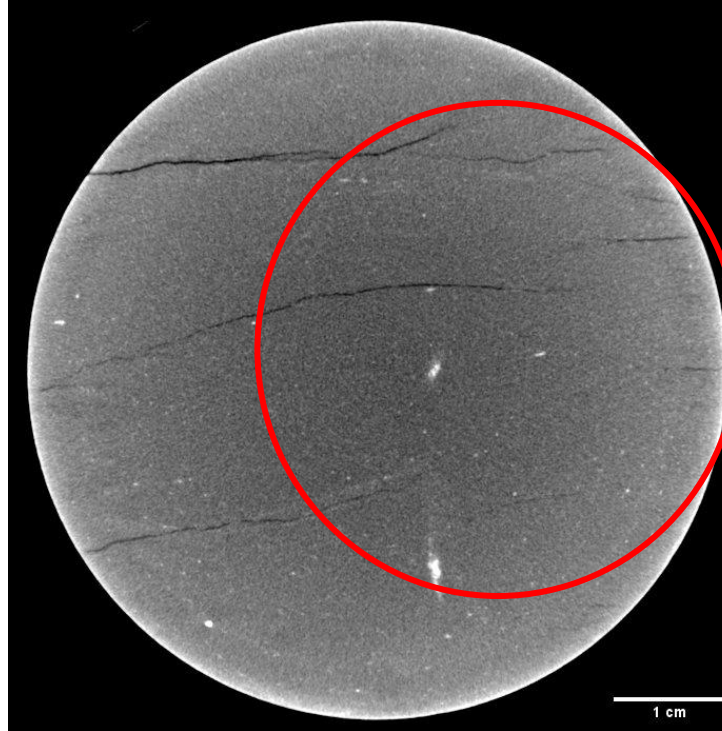
# Fracture Network Analysis



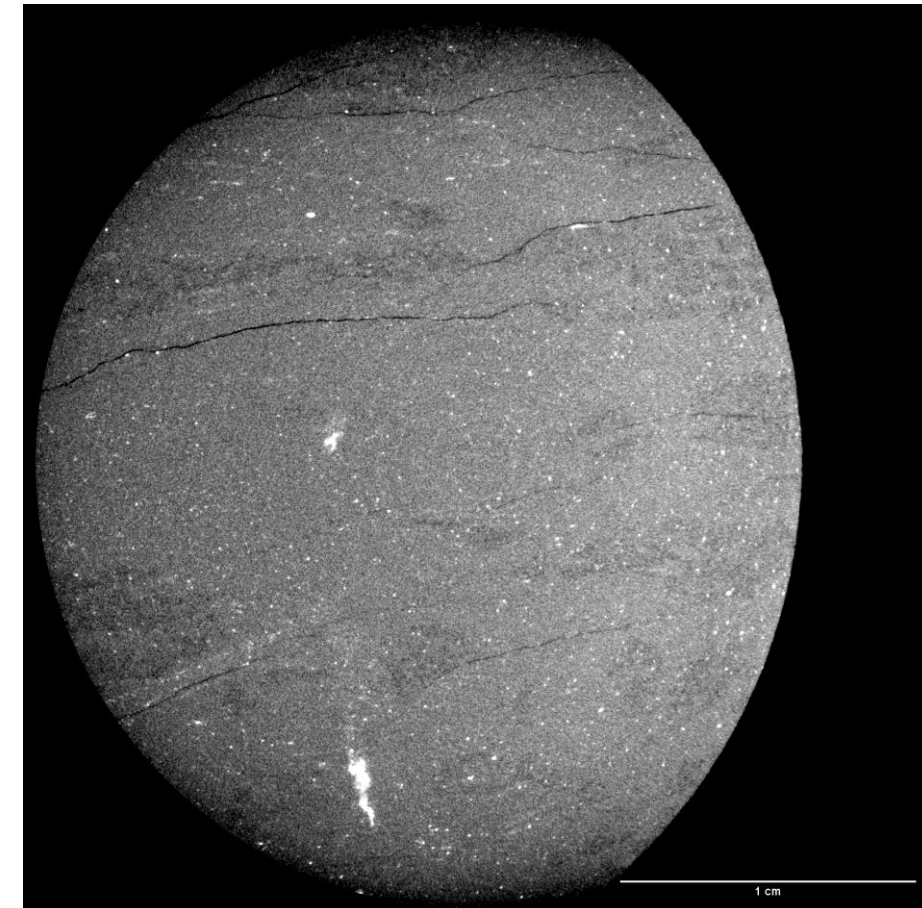
Xenon Infiltration  
At 1100 PSI Effective



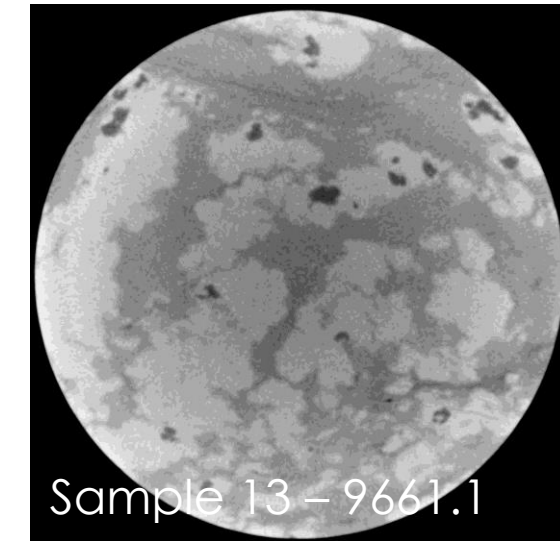
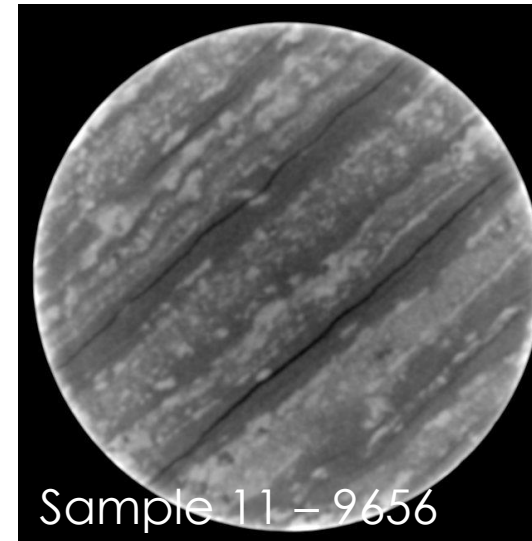
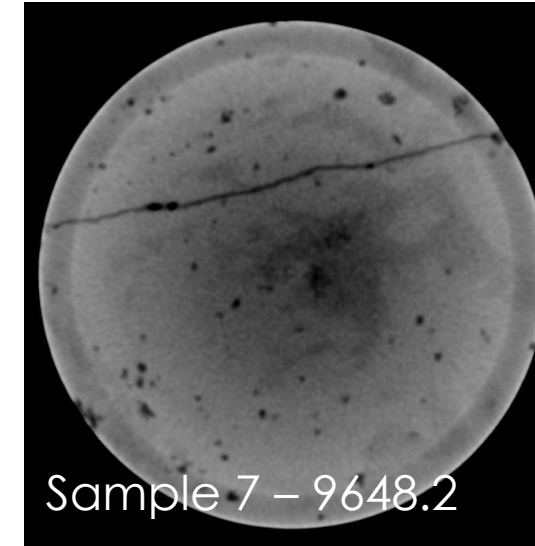
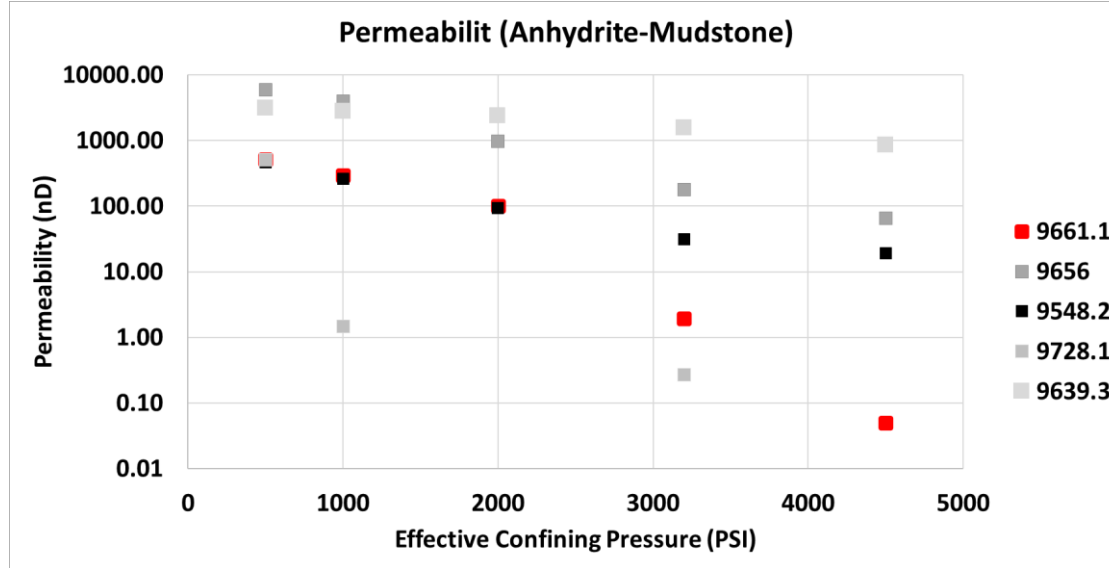
DynaTOM Whole Core plug



DynaTOM high resolution



# What Might this Mean in Anhydrite Dolomudstone?



- Samples are heterogeneous in their distribution of mudstone and continuity of dolomite/anhydrite.
- Samples with a linear decline appear to have pre-existing fractures and XRF results show less Mg, suggesting less dolomite.

# Conclusions:

---



- The 110 ft of core from the State 16-2 well was scanned in the CT scanner and the MSCL at 6 cm resolution. The high resolution XRF data was used to differentiate three lithofacies (Halite, Anhydrite-rich zone, Mudstone/sandy-siltstone).
- The sandy-siltstone/mudstone samples showed a rapid decline in permeability followed by a linear decrease; whereas the anhydrite-mudstone samples showed a linear decrease in permeability with increasing effective confining pressure.
- Samples 13 and 60 showed a more rapid drop off in permeability, which is likely due to permeability drivers in mudstone fractures rather than in the anhydrite/dolomite.
- Xenon flood shows fracture network is primarily focused within open fractures at high effective confining pressures, and the addition of prominent, non-uniform matrix diffusion of Xe at 1,100 psi effective pressure.
  - This is likely a combination of edge damage and mineralogical changes, future investigation of higher resolution images should help to resolve this.

# Acknowledgments

---



**This work was completed at the National Energy Technology Laboratory (NETL) with support from U.S. Department of Energy's (DOE) Office of Fossil Energy Oil & Gas Program.**

The author would like to thank Bryan Tenant, Karl Jarvis, and Scott Workman for data collection and technical support. This research was supported in part by appointments from the NETL Research Participation Program, sponsored by the U.S. DOE and administered by the Oak Ridge Institute for Science and Education.

# NETL RESOURCES

---

VISIT US AT: [www.NETL.DOE.gov](http://www.NETL.DOE.gov)

 @NETL\_DOE

 @NETL\_DOE

 @NationalEnergyTechnologyLaboratory

